Planta (2020) 251:40
https://doi.org/10.1007/s00425-019-03332-x

SHORT COMMUNICATION

Identification of two oxygenase genes involved in the respective biosynthetic pathways of canonical and non-canonical strigolactones in *Lotus japonicus*

Narumi Mori[1] · Takahito Nomura[2] · Kohki Akiyama[1]

Received: 14 November 2019 / Accepted: 20 December 2019 / Published online: 6 January 2020

Abstract

Main conclusion **A cytochrome P450 and a 2-oxoglutarate-dependent dioxygenase genes responsible, respectively, for the biosyntheses of canonical and non-canonical strigolactones in *Lotus japonicus* were identified by transcriptome profiling and mutant screening.**

Abstract Strigolactones (SLs) are a group of apocarotenoids with diverse structures that act as phytohormones and rhizosphere signals. The model legume *Lotus japonicus* produces both canonical and non-canonical SLs, 5-deoxystrigol (5DS) and lotuslactone (LL), respectively, through oxidation of a common intermediate carlactone by the cytochrome P450 (CYP) enzyme MAX1. However, the pathways downstream of MAX1 and the branching point in the biosyntheses of 5DS and LL have not been elucidated. Here, we identified a CYP and a 2-oxoglutarate-dependent dioxygenase (2OGD) genes responsible, respectively, for the formation of *Lotus* SLs by transcriptome profiling using RNA-seq and screening of SL-deficient mutants from the *Lotus retrotransposon 1* (*LORE1*) insertion mutant resource. The CYP and 2OGD genes were named *DSD* and *LLD*, respectively, after 5DS or LL defective phenotype of the mutants. The involvements of the genes in *Lotus* SL biosyntheses were confirmed by restoration of the mutant phenotype using *Agrobacterium rhizogenes*-mediated transformation to generate transgenic roots expressing the coding sequence. The transcript levels of *DSD* and *LLD* in roots as well as the levels of 5DS and LL in root exudates were reduced by phosphate fertilization and gibberellin treatment. This study can provide the opportunity to investigate how and why plants produce the two classes of SLs.

Keywords Arbuscular mycorrhizal fungi · Cytochrome P450 · 5-Deoxystrigol · Lotuslactone · 2-Oxoglutarate-dependent dioxygenase · Root parasitic plants

Abbreviations

CLA	Carlactonoic acid
CYP	Cytochrome P450
DSD	5-Deoxystrigol defective
5DS	5-Deoxystrigol
LL	Lotuslactone
LLD	Lotuslactone defective
LORE1	Lotus retrotransposon 1
MAX1	MORE AXILLARY GROWTH 1
2OGD	2-Oxoglutarate-dependent dioxygenase
SLs	Strigolactones

Electronic supplementary material The online version of this article (https://doi.org/10.1007/s00425-019-03332-x) contains supplementary material, which is available to authorized users.

✉ Kohki Akiyama
akiyama@biochem.osakafu-u.ac.jp

[1] Department of Applied Life Sciences, Graduate School of Life and Environmental Sciences, Osaka Prefecture University, 1-1 Gakuen-cho, Nakaku, Sakai, Osaka 599-8531, Japan

[2] Center for Bioscience Research and Education, Utsunomiya University, Utsunomiya 321-8505, Japan

Introduction

Strigolactones (SLs) are a class of phytohormones that also act as rhizosphere signals for arbuscular mycorrhizal fungi and root parasitic plants (Al-Babili and Bouwmeester 2015). To date, approximately 30 SLs have been characterized from various plant species (Yoneyama et al. 2018b). Natural SLs consist of an (*R*)-configurated

butenolide ring (D-ring) linked by an enol ether bridge to a less conserved second moiety (Jia et al. 2018; Wang and Bouwmeester 2018). SLs are classified into two groups, canonical and non-canonical SLs, based on the structure of the second moieties. Canonical SLs possess a tricyclic lactone ring (ABC ring), while non-canonical SLs lack the A, B, or C ring. Canonical SLs are further divided into strigol- and orobanchol-type SLs, which have an α- and a β-oriented C ring, respectively (Fig. 1a).

SL biosynthesis is initiated from the conversion of β-carotene to carlactone by the sequential action of DWARF27, CAROTENOID CLEAVAGE DIOXYGENASE 7 and CAROTENOID CLEAVAGE DIOXYGENASE 8 (Alder et al. 2012; Seto et al. 2014). In *Arabidopsis*, carlactone is converted by the cytochrome P450 (CYP) enzyme MORE AXILLARY GROWTH 1 (MAX1) (CYP711A) into carlactonoic acid (CLA) that is methylated to methyl carlactonoate (Abe et al. 2014). Methyl carlactonoate is oxygenated by the 2-oxoglutarate-dependent dioxygenase (2OGD) enzyme LATERAL BRANCHING OXIDOREDUCTASE (LBO), to an unidentified SL-like compound (Brewer et al. 2016). In rice, one of MAX1 homologs, Os900, converts carlactone to an orobanchol-type SL, 4-deoxyorobanchol, and another MAX1 homolog, Os1400, hydroxylates 4-deoxyorobanchol to orobanchol (Zhang et al. 2014). The conversion of carlactone to CLA is a common reaction catalyzed by MAX1 homologs as found recently (Yoneyama et al. 2018a). In sorghum, a sulfotransferase, LOW GERMINATION STIMULANT 1, is likely to be involved in a strigol-type SL, 5-deoxystrigol (5DS) production (Gobena et al. 2017).

The model legume *Lotus japonicus* produces canonical 5DS that was isolated as the first hyphal branching factor for arbuscular mycorrhizal fungi (Fig. 1a) (Akiyama et al. 2005). Non-canonical lotuslactone (LL) is the second branching factor identified in *L. japonicus* (Fig. 1a) (Xie et al. 2019). Despite that 5DS is considerably more active than LL in hyphal branching (Akiyama et al. 2010), *L. japonicus* roots exude both SLs (Xie et al. 2019). LL lacks the C-ring and has a seven-membered cycloheptadiene A-ring as in medicaol (Tokunaga et al. 2015). Its B-ring is highly oxygenated with hydroxy, acetyloxy, and oxo groups. The large structural difference between 5DS and LL implies that these two SLs are produced by branched biosynthetic pathways. Recently, we showed that LjMAX1 (CYP711A9) catalyzes the oxidation of carlactone to 18-hydroxyCLA via CLA, and that 18-hydroxylated carlactonoates are common biosynthetic precursors for 5DS and LL in *L. japonicus* (Mori et al. 2019). In addition, the *ljmax1* mutant was deficient in both 5DS and LL. These findings indicate that the branching point in the biosynthesis of 5DS and LL is positioned downstream of LjMAX1. However, nothing is known about the pathways

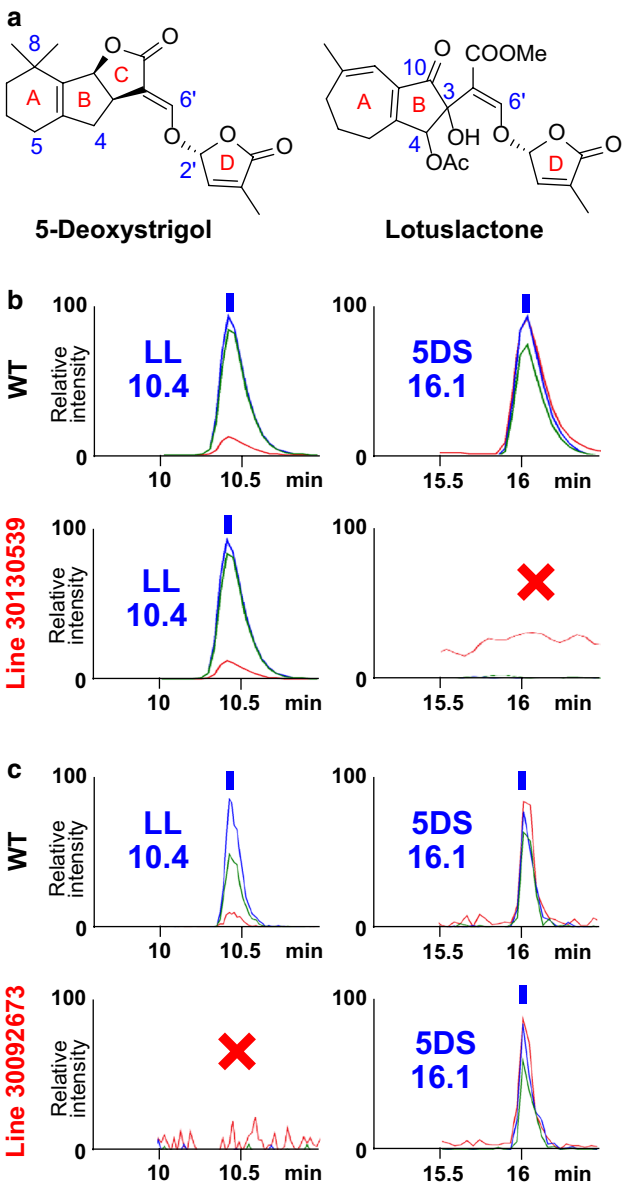

Fig. 1 *Lotus* SLs production of WT and the candidate gene mutants were analyzed by LC–MS/MS. **a** Structures of *L. japonicus* SLs. 5-Deoxystrigol (5DS) is a canonical SL possessing a tricyclic lactone ring (ABC ring). Lotuslactone (LL) is a non-canonical SL lacking C ring. **b** 5DS and LL in root exudates of WT and line 30130539 (*dsd*) were analyzed. **c** 5DS and LL in root exudates of WT and line 30092673 (*lld*) were analyzed. MRM chromatograms of 5DS (the precursor ion $[M+H]^+$, red: 331.15/216.00, blue: 331.15/97.00, green: 331.15/234.00, *m/z* in positive mode) and LL (the precursor ion $[M\text{-}AcO+H]^+$, red: 373.00/276.00, blue: 373.00/244.00, green: 373.00/216.00, *m/z* in positive mode) are shown

downstream of MAX1 and the branching point to produce 5DS and LL in *L. japonicus*.

In this study, we attempted to discover novel genes encoding enzymes involved in the individual biosynthetic pathways of 5DS and LL in *L. japonicus*. The pathway from

18-hydroxyCLA to 5DS is expected to include oxidative cyclization step(s) in the BC ring formation as observed for Os900. The same is likely true for the B ring formation in LL biosynthesis. In addition, the construction of LL requires ring expansion in the A-ring and substitution of oxygenated functionalities in the B-ring. We, therefore, focused on genes encoding CYP and 2OGD enzymes as candidates involved in such processes. The results we report here are the identification of a CYP and a 2OGD genes responsible, respectively, for the biosyntheses of *Lotus* SLs by transcriptome profiling and mutant screening, and their transcriptional responses to phosphorus availability and a phytohormone gibberellin.

Materials and methods

Plant growth and treatment

Lotus japonicus L. ecotype Gifu B-129 provided by the National BioResource Project (*L. japonicus* and *Glycine max*; https://www.legumebase.brc.miyazaki-u.ac.jp/index.jsp) was used as the WT. *LORE1* mutants were obtained from the *LORE1* insertion mutant resource (Fukai et al. 2012; Urbański et al. 2012). Genotyping of *LORE1* mutants was performed using primers listed in Supplementary Table S1. Seedlings were grown hydroponically as described previously (Mori et al. 2019). Phosphate and gibberellin treatments and CLA feeding were performed using shaded centrifuge tubes (50 ml) containing 40 ml hydroponic solutions.

Liquid chromatography-tandem mass spectrometry (LC–MS/MS) analysis

Measurements of SL levels in root exudates were performed with UHPLC (Nexera X2, Shimadzu) and an ion trap instrument (amaZon SL, Bruker) using authentic standards as described previously (Yoneyama et al. 2018a; Mori et al. 2019).

RNA-sequencing (RNA-seq)

Sequencing library construction and RNA-seq on an Illumina HiSeq 2000 sequencer (paired-end, 100 bp) were performed by Macrogen Japan (Kyoto, Japan) using total RNA extracted from roots using an RNeasy Plant Mini Kit (Qiagen).

Cloning

Total RNA was extracted from roots of the WT using an RNeasy Plant Mini Kit (Qiagen). The first strand cDNA was synthesized using SMARTScribe Reverse Transcriptase included in a SMARTer rapid amplification of cDNA ends (RACE) 5′/3′ Kit (Clontech). 5′- and 3′-RACE to obtain partial sequences of *DSD* were performed using the kit with 5′-UTR-GSP2 and 3′-UTR-GSP1 primers (Supplementary Table S2). The full-length coding sequences were amplified from the first strand cDNA by nested-polymerase chain reaction (PCR) using PrimeSTAR Max DNA polymerase (Takara) with the first primers 5′-UTR-*DSD/LLD*-F and 3′-UTR-*DSD/LLD*-R and the second primers Nested-5′-UTR-*DSD/LLD*-F and Nested-3′-UTR-*DSD/LLD*-R. The full-length cDNAs were subcloned into the cloning vector pTAC1 (DynaExpress) for sequencing or the expression vector pUB-GW-GFP for *Agrobacterium*-mediated transformation (Maekawa et al. 2008) by an In-Fusion HD Cloning Kit (Takara) using INF-*DSD/LLD*-F and INF-*DSD/LLD*-R primers. Sequencing was performed by Eurofins Genomics (Tokyo, Japan) using the Sanger method. The phylogenetic tree was constructed using the MEGA7 program (Kumar et al. 2016). The homologous sequences of *DSD* and *LLD* in representative plant species were obtained from Phytozome v12.1 (https://phytozome.jgi.doe.gov/pz/portal.html).

Agrobacterium rhizogenes-mediated transformation

LORE1 mutants were transformed by *A. rhizogenes* strain AR1193 harboring pUB-GW-*DSD*-GFP, pUB-GW-*LLD*-GFP, or pUB-GW-GFP according to the method of Okamoto et al. (2013). Composite plants consisting of transformed hairy roots expressing GFP were used for further analysis.

Quantitative reverse-transcriptase PCR (qRT-PCR) analysis

Total RNA extracted from roots as above was treated by TURBO DNA-free Kit (Ambion), and reverse transcribed using a High-Capacity RNA-to-cDNA Kit (Applied Biosystems). qRT-PCR was performed on an ABI PRISM 7300 sequence detection system using a Power SYBR Green PCR Master Mix (Applied Biosystems) with primers listed in Supplementary Table S3. Ubiquitin4 expression was used as an internal standard.

Statistical analysis

Student's *t*-test was applied to evaluate the significance of the results obtained.

Accession number

The accession numbers of the *DSD* and *LLD* sequences are LC508723 and LC508724, respectively.

Results and discussion

In general, SL production is promoted by phosphate (Pi) starvation (Umehara et al. 2010; Yamada et al. 2014). By contrast, the supply of Pi negatively regulates SL levels in roots and root exudates with a concomitant downregulation of multiple SL biosynthetic genes (Umehara et al. 2010; Liu et al. 2015; Zhang et al. 2018). To check the Pi-dependent change in SL levels in *L. japonicus*, we quantified SL levels in root exudates of seedlings continuously starved or supplied with Pi by LC–MS/MS analysis (Supplementary Fig. S1a). The levels of 5DS and LL in Pi-supplied seedlings were significantly decreased to 7.5% and 4.7% of continuously Pi-starved control, respectively (Supplementary Fig. S1b). To screen candidate oxygenase genes involved in the biosyntheses of *Lotus* SLs, we performed transcriptome profiling by RNA-seq on roots of Pi-starved or supplied seedlings grown under the same conditions as above (Supplementary Table S4). Among 655 genes annotated as CYP (473 genes) and 2OGD (182 genes) in the *L. japonicus* genome database, 49% of genes (CYP 224 genes, 2OGD 99 genes) were downregulated in Pi supplied roots compared to Pi starved roots. These downregulated oxygenase genes were ranked in descending order based on the degree of expression change. To identify genes responsible for the biosyntheses of 5DS and/or LL, we next performed a screen for SL-defect mutants from the *LORE1* insertion mutant resource (Fukai et al. 2012; Urbański et al. 2012). We retrieved *LORE1* mutant lines containing exonic insertions in the higher ranked genes through Lotus Base (https://lotus.au.dk). The homozygous *LORE1* mutants were grown hydroponically without Pi, and analyzed for SL production in root exudates. Through a screen of the top 29 candidates, we found that two mutant lines 30130539 and 30092673 were defect, respectively, in 5DS and LL production. Both SLs were detected in root exudates of the WT. Only LL was detected in line 30130539 homozygous for a putative CYP gene Lj0g3v0346399 (Fig. 1b). We named this gene *DSD* after 5DS-defective phenotype. Only 5DS was detected in line 30092673 homozygous for a putative 2OGD gene Lj1g3v4997280 (Fig. 1c). We named this gene *LLD* after LL-defective phenotype.

The coding sequence (CDS) of *DSD* and *LLD* genes were cloned from cDNA of the WT ecotype Gifu B-129. Based on the partial coding sequence available, the missing cDNA sequences were obtained by 5′- and 3′-RACE. Using protein sequences encoding these DNA fragments as query, OrthoDB (https://www.orthodb.org/) searches were performed against *Medicago truncatula* and *Glycine max*. By comparing the gene sequences of orthologs in *M. truncatula* and *G. max*, we predicted the full-length mRNA sequences of *DSD* and *LLD*, and designed 5′-untranslated region (UTR) and 3′-UTR primers. The full-length CDSs of the two genes were obtained by PCR using the primer sets. The CDSs of *DSD* and *LLD* were 1455 bp encoding for a 484-amino acid protein, and 1071 bp encoding for a 356-amino acid protein, respectively (Supplementary Table S5). Phylogenetic analysis revealed that *DSD* belongs to CYP722C subfamily (Nelson et al. 2008) (Supplementary Fig. S2). Other legumes have both CYP722A and CYP722C, while *Arabidopsis* and gramineous plants have only CYP722A and CYP722B, respectively. *LLD* falls within the DOXC55 clade of 2OGDs as shown by a phylogenetic tree (Kawai et al. 2014) (Supplementary Fig. S3). The next clade DOXC54 includes *LBO*.

In the *dsd* mutant, the *LORE1* retroelement was inserted in the first exon, 66 bp after the start codon of *DSD* in contig CM0131 on chromosome 4 (in build 2.5) (Fig. 2a). In the *lld* mutant, the *LORE1* retroelement was inserted in the second exon, 357 bp after the start codon of *LLD* (Gene ID

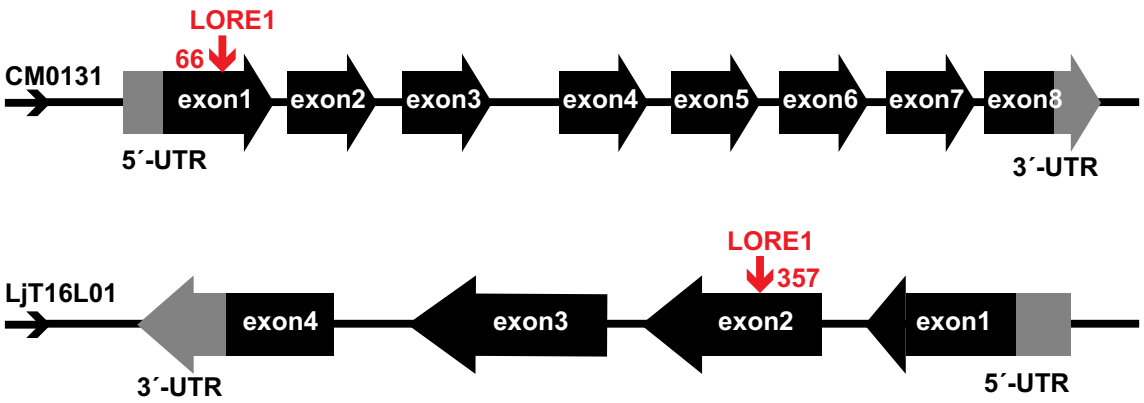

Fig. 2 Location of the *LORE1* insertion in *DSD* and *LLD* genes. **a** *DSD* locates in contig CM0131 on chromosome 4 and has eight exons. The *dsd* mutant has the *LORE1* retroelement in the first exon. **b** *LLD* locates in contig LjT16L01 on chromosome 4 and has four exons. The *lld* mutant has the *LORE1* retroelement in the second exon

chr4.LjT16L01.240.r2.d in build 2.5) in contig LjT16L01 on chromosome 4 (Fig. 2b). To directly confirm the involvement of *DSD* and *LLD* in 5DS or LL-defective phenotype of the mutants, we used *A. rhizogenes*-mediated transformation to generate transgenic roots expressing the WT cDNA sequence. The full-length CDSs were cloned behind the *LjUBIQUITIN* promoter in the vector pUB-GW-GFP. The constructs were introduced into roots of the mutants by *A. rhizogenes* harboring the vectors. 5DS was not detected in root exudates of *dsd* transformed with empty vector, while 5DS production was restored in transformed *dsd* harboring the *DSD* CDS (Fig. 3a). Likewise, LL was not detected in root exudates of *lld* transformed with empty vector, while LL production was restored in those transformed with pUB-GW-*LLD*-GFP (Fig. 3b). Taken together, we demonstrated that the exonic mutations in *DSD* and *LLD* genes caused SL deficiency in the mutants.

To check the Pi-dependent change in transcript levels of *DSD* and *LLD* as well as other known SL biosynthetic genes, we analyzed their transcript levels by qRT-PCR in the WT roots grown under the same condition in the RNA-seq analysis as above. Our analysis revealed that the supply of Pi reduced transcript levels of the SL biosynthetic genes, *LjD27, LjCCD7, LjCCD8*, *LjMAX1*, *DSD* and *LLD*, but did not affect that of the SL signaling gene *D14* (Supplementary Fig. S4). It was recently discovered that gibberellin signaling negatively regulates SL biosynthesis in rice and *Arabidopsis* (Ito et al. 2017; Lantzouni et al. 2017). We investigated whether the same mechanism is involved in the regulation of SL biosynthesis in *L. japonicus* using the WT seedlings grown with or without active gibberellic acid (GA_3) in the hydroponic solutions. GA_3 treatment reduced not only transcript levels of *LjCCD7, LjCCD8*, *LjMAX1*, *DSD* and *LLD* in roots but also 5DS and LL levels in root exudates (Supplementary Fig. S5). These results showed that SL biosynthesis is negatively regulated by phosphate and gibberellin in *L. japonicus*.

We performed feeding experiments with exogenous CLA using *dsd* and analyzed labeled products in root exudates by LC–MS/MS. We could not detect the peak of labeled 5DS, but could detect 18-hydroxyCLA, indicating that DSD is an enzyme in the later stage of 5DS biosynthesis downstream of LjMAX1 and its enzymatic function was not C-18 hydroxylation of CLA (Supplementary Fig. S6).

In conclusion, we identified novel oxygenase genes *DSD* and *LLD* involved, respectively, in the biosyntheses of canonical 5DS and non-canonical LL in *L. japonicus*. Further characterization of DSD and LLD enzymes, including identification of substrates and products, will advance our understanding of SL biosynthetic pathway. The availability of the *dsd* and *lld* mutants will provide the opportunity to assess the functional differences between canonical and non-canonical SLs in rhizosphere signaling. These studies will

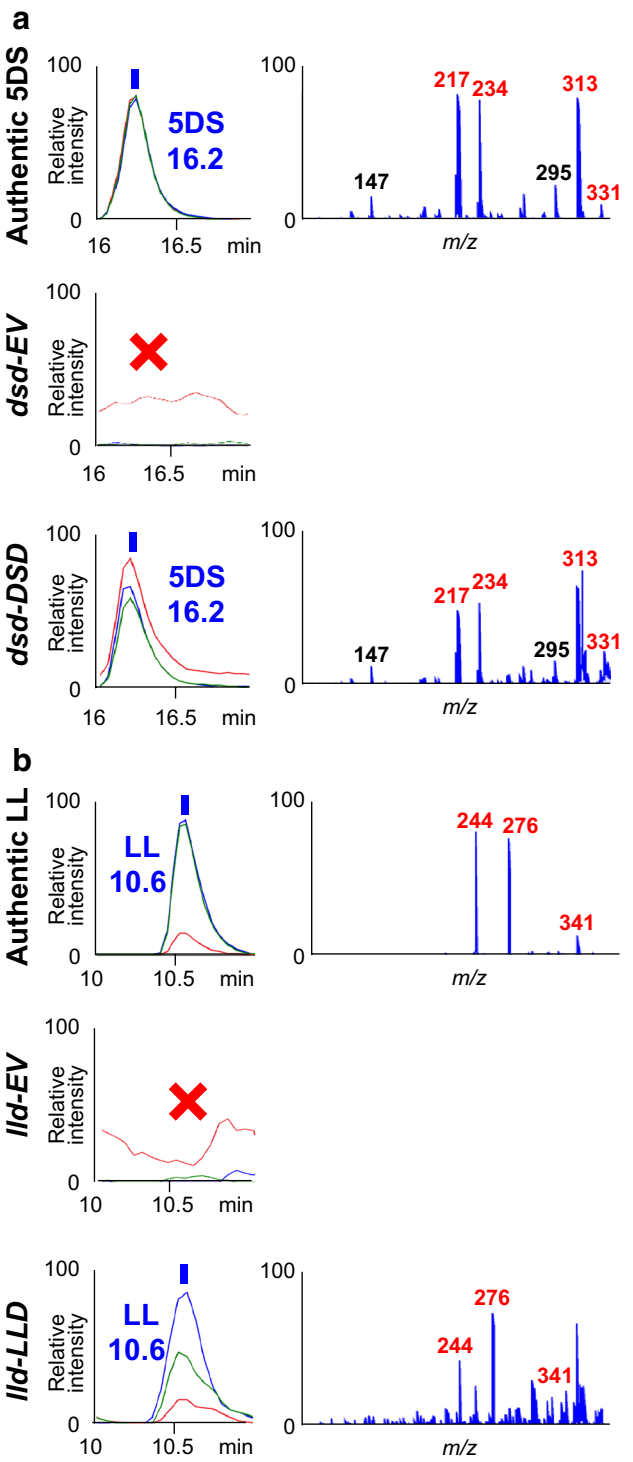

Fig. 3 Restoration of *Lotus* SLs production in the *LORE1* insertion mutants expressing the WT cDNA sequence by *A. rhizogenes*-mediated hairy root transformation. Root exudates and authentic standards were analyzed by LC–MS/MS. **a** *dsd* was transformed by pUB-GW-*DSD*-GFP (*dsd-DSD*) and pUB-GW-GFP (empty vector, *dsd*-EV). **b** *lld* was transformed by pUB-GW-*LLD*-GFP (*lld-LLD*) and pUB-GW-GFP (empty vector, *lld*-EV). MRM chromatograms (left) and full-scan spectra of fragment ions (right). MRM chromatograms of 5DS (the precursor ion $[M+H]^+$, red: 331.15/216.00, blue: 331.15/97.00, green: 331.15/234.00, *m/z* in positive mode) and LL (the precursor ion $[M\text{-}AcO+H]^+$, red: 373.00/276.00, blue: 373.00/244.00, green: 373.00/216.00, *m/z* in positive mode) are shown

provide insights into how and why plants produce the two classes of SLs.

Author Contribution Statement NM and KA conceived and designed research. NM conducted experiments. NM, TN and KA analyzed data. NM and KA wrote the manuscript. All authors read and approved the manuscript.

Acknowledgements We thank Masayoshi Kawaguchi (National Institute for Basic Biology) for providing *Agrobacterium rhizogenes* AR1193, and Hiromu Kameoka (Osaka Prefecture University) for discussion on RNA-Seq analysis. This work was supported by the Science and Technology Research Promotion Program for Agriculture, Forestry, Fisheries and Food Industry, and Grant-in-Aid for JSPS Fellows [Grant Number 17J05519].

References

Abe S, Sado A, Tanaka K et al (2014) Carlactone is converted to carlactonoic acid by MAX1 in *Arabidopsis* and its methyl ester can directly interact with AtD14 in vitro. Proc Natl Acad Sci USA 111:18084–18089. https://doi.org/10.1073/pnas.1410801111

Akiyama K, Matsuzaki KI, Hayashi H (2005) Plant sesquiterpenes induce hyphal branching in arbuscular mycorrhizal fungi. Nature 435:824–827. https://doi.org/10.1038/nature03608

Akiyama K, Ogasawara S, Ito S, Hayashi H (2010) Structural requirements of strigolactones for hyphal branching in AM fungi. Plant Cell Physiol 51:1104–1117. https://doi.org/10.1093/pcp/pcq058

Al-Babili S, Bouwmeester HJ (2015) Strigolactones, a novel carotenoid-derived plant hormone. Annu Rev Plant Biol 66:161–186. https://doi.org/10.1146/annurev-arplant-043014-114759

Alder A, Jamil M, Marzorati M et al (2012) The path from β-carotene to carlactone, a strigolactone-like plant hormone. Science 335:1348–1351. https://doi.org/10.1126/science.1218094

Brewer PB, Yoneyama K, Filardo F et al (2016) LATERAL BRANCHING OXIDOREDUCTASE acts in the final stages of strigolactone biosynthesis in *Arabidopsis*. Proc Natl Acad Sci USA 113:6301–6306. https://doi.org/10.1073/pnas.1601729113

Fukai E, Soyano T, Umehara Y et al (2012) Establishment of a *Lotus japonicus* gene tagging population using the exon-targeting endogenous retrotransposon *LORE1*. Plant J 69:720–730. https://doi.org/10.1111/j.1365-313X.2011.04826.x

Gobena D, Shimels M, Rich PJ et al (2017) Mutation in sorghum *LOW GERMINATION STIMULANT 1* alters strigolactones and causes *Striga* resistance. Proc Natl Acad Sci USA 114:4471–4476. https://doi.org/10.1073/pnas.1618965114

Ito S, Yamagami D, Umehara M et al (2017) Regulation of strigolactone biosynthesis by gibberellin signaling. Plant Physiol 174:1250–1259. https://doi.org/10.1104/pp.17.00301

Jia K-P, Baz L, Al-Babili S (2018) From carotenoids to strigolactones. J Exp Bot 69:2189–2204. https://doi.org/10.1093/jxb/erx476

Kawai Y, Ono E, Mizutani M (2014) Evolution and diversity of the 2-oxoglutarate-dependent dioxygenase superfamily in plants. Plant J 78:328–343. https://doi.org/10.1111/tpj.12479

Kumar S, Stecher G, Tamura K (2016) MEGA7: Molecular evolutionary genetics analysis version 7.0 for bigger datasets. Mol Biol Evol 33:1870–1874. https://doi.org/10.1093/molbev/msw054

Lantzouni O, Klermund C, Schwechheimer C (2017) Largely additive effects of gibberellin and strigolactone on gene expression in *Arabidopsis thaliana* seedlings. Plant J 92:924–938. https://doi.org/10.1111/tpj.13729

Liu J, He H, Vitali M et al (2015) Osmotic stress represses strigolactone biosynthesis in *Lotus japonicus* roots: exploring the interaction between strigolactones and ABA under abiotic stress. Planta 241:1435–1451. https://doi.org/10.1007/s00425-015-2266-8

Maekawa T, Kusakabe M, Shimoda Y, Sato S, Tabata S, Murooka Y, Hayashi M (2008) Polyubiquitin promoter-based binary vectors for overexpression and gene silencing in *Lotus japonicus*. Mol Plant Microbe Interact 21:375–382. https://doi.org/10.1094/MPMI-21-4-0375

Mori N, Sado A, Xie X, et al (2019) Chemical identification of 18-hydroxycarlactonoic acid as an LjMAX1 product and conversion of 18-hydroxylcarlactonoates to canonical and non-canonical strigolactones in *Lotus japonicus*. bioRxiv 837708. Doi: 10.1101/837708

Nelson DR, Ming R, Alam M, Schuler MA (2008) Comparison of cytochrome P450 genes from six plant genomes. Trop Plant Biol 1:216–235. https://doi.org/10.1007/s12042-008-9022-1

Okamoto S, Yoro E, Suzaki T, Kawaguchi M (2013) Hairy root transformation in *Lotus japonicus*. Bio-Protocol 3: e795. doi: 10.21769/BioProtoc.795

Seto Y, Sado A, Asami K et al (2014) Carlactone is an endogenous biosynthetic precursor for strigolactones. Proc Natl Acad Sci USA 111:1640–1645. https://doi.org/10.1073/pnas.1314805111

Tokunaga T, Hayashi H, Akiyama K (2015) Medicaol, a strigolactone identified as a putative didehydro-orobanchol isomer, from *Medicago truncatula*. Phytochemistry 111:91–97. https://doi.org/10.1016/J.PHYTOCHEM.2014.12.024

Umehara M, Hanada A, Magome H et al (2010) Contribution of strigolactones to the inhibition of tiller bud outgrowth under phosphate deficiency in rice. Plant Cell Physiol 51:1118–1126. https://doi.org/10.1093/pcp/pcq084

Urbański DF, Małolepszy A, Stougaard J, Andersen SU (2012) Genome-wide *LORE1* retrotransposon mutagenesis and high-throughput insertion detection in *Lotus japonicus*. Plant J 69:731–741. https://doi.org/10.1111/j.1365-313X.2011.04827.x

Wang Y, Bouwmeester HJ (2018) Structural diversity in the strigolactones. J Exp Bot 69:2219–2230. https://doi.org/10.1093/jxb/ery091

Xie X, Mori N, Yoneyama K et al (2019) Lotuslactone, a non-canonical strigolactone from *Lotus japonicus*. Phytochemistry 157:200–205. https://doi.org/10.1016/J.PHYTOCHEM.2018.10.034

Yamada Y, Furusawa S, Nagasaka S et al (2014) Strigolactone signaling regulates rice leaf senescence in response to a phosphate deficiency. Planta 240:399–408. https://doi.org/10.1007/s00425-014-2096-0

Yoneyama K, Mori N, Sato T et al (2018a) Conversion of carlactone to carlactonoic acid is a conserved function of MAX1 homologs in strigolactone biosynthesis. New Phytol 218:1522–1533. https://doi.org/10.1111/nph.15055

Yoneyama K, Xie X, Yoneyama K et al (2018b) Which are major players, canonical or non-canonical strigolactones? J Exp Bot 69:2231–2239. https://doi.org/10.1093/jxb/ery090

Zhang Y, van Dijk ADJ, Scaffidi A et al (2014) Rice cytochrome P450 MAX1 homologs catalyze distinct steps in strigolactone biosynthesis. Nat Chem Biol 10:1028–1033. https://doi.org/10.1038/nchembio.1660

Zhang Y, Cheng X, Wang Y et al (2018) The tomato *MAX1* homolog, *SlMAX1*, is involved in the biosynthesis of tomato strigolactones from carlactone. New Phytol 219:297–309. https://doi.org/10.1111/nph.15131